Functional Characterization of Homo- and Heteromeric Channel Kinases TRPM6 and TRPM7

Mingjiang Li,[1,2] Jianmin Jiang,[1] and Lixia Yue[1]

[1]Center for Cardiology and Cardiovascular Biology, Department of Cell Biology, University of Connecticut Health Center, Farmington, CT 06030

[2]Department of Cardiology, Renmin Hospital of Wuhan University, 430060, People's Republic of China

TRPM6 and TRPM7 are two known channel kinases that play important roles in various physiological processes, including Mg^{2+} homeostasis. Mutations in TRPM6 cause hereditary hypomagnesemia and secondary hypocalcemia (HSH). However, whether TRPM6 encodes functional channels is controversial. Here we demonstrate several signature features of TRPM6 that distinguish TRPM6 from TRPM7 and TRPM6/7 channels. We show that heterologous expression of TRPM6 but not the mutant $TRPM6^{S141L}$ produces functional channels with divalent cation permeability profile and pH sensitivity distinctive from those of TRPM7 channels and TRPM6/7 complexes. TRPM6 exhibits unique unitary conductance that is 2- and 1.5-fold bigger than that of TRPM7 and TRPM6/7. Moreover, micromolar levels of 2-aminoethoxydiphenyl borate (2-APB) maximally increase TRPM6 but significantly inhibit TRPM7 channel activities; whereas millimolar concentrations of 2-APB potentiate TRPM6/7 and TRPM7 channel activities. Furthermore, Mg^{2+} and Ca^{2+} entry through TRPM6 is enhanced three- to fourfold by 2-APB. Collectively, these results indicate that TRPM6 forms functional homomeric channels as well as heteromeric TRPM6/7 complexes. The unique characteristics of these three channel types, TRPM6, TRPM7, and TRPM6/7, suggest that they may play different roles in vivo.

The Journal of General Physiology

INTRODUCTION

TRPM6 and TRPM7 are unique channel kinases that belong to the long or melastatin-related transient receptor potential TRPM subfamily of TRP channel superfamily (Harteneck et al., 2000; Clapham, 2003; Fleig and Penner, 2004; Schmitz et al., 2004; Montell, 2005). Recent studies have indicated that TRPM6 and TRPM7 play important physiological roles (Nadler et al., 2001; Schlingmann et al., 2002; Walder et al., 2002; Schmitz et al., 2003; Hanano et al., 2004; Elizondo et al., 2005; Hermosura et al., 2005; Nilius et al., 2005; Schlingmann et al., 2005). Mutations of TRPM6 cause inherited hypomagnesemia and secondary hypocalcemia (HSH) (Walder et al., 2002; Schlingmann and Gudermann, 2005; Schlingmann et al., 2002, 2005), while mutation of TRPM7 may contribute to the pathogenesis of Guamanian neurodegenerative disorders (Hermosura et al., 2005). Furthermore, TRPM7 appears to be essential for cell viability and growth (Nadler et al., 2001; Schmitz et al., 2003; Hanano et al., 2004; Elizondo et al., 2005), whereas overwhelming Ca^{2+} entry through TRPM7 is involved in anoxic neuronal cell death (Aarts et al., 2003).

TRPM6 and TRPM7 are close homologues and the only known ion channels with an intrinsic kinase domain. Unlike the ubiquitously expressed TRPM7, TRPM6 is mainly distributed in kidney and small intestine (Schlingmann et al., 2002; Walder et al., 2002). In contrast to TRPM7, whose functional properties have been extensively investigated, the experimental findings for TRPM6 are controversial (Chubanov et al., 2004; Voets et al., 2004; Schlingmann and Gudermann, 2005). Voets and colleagues successfully expressed functional TRPM6 channels in HEK-293 cells and demonstrated similar properties of TRPM6 to those of TRPM7 (Voets et al., 2004). In contrast, Chubanov et al. (2004) reported that in HEK-293 cells and *Xenopus* oocytes, TRPM6 does not produce functional currents by itself. Instead, TRPM7 is required for TRPM6 to incorporate into channel complexes at the plasma membrane. The association of TRPM6 and TRPM7 channel proteins is also demonstrated in a recent study (Schmitz et al., 2005), although the detailed functional characteristics of TRPM6/7 channels remain unknown (Chubanov et al., 2005). Given the potential importance of TRPM6 and TRPM7 in Mg^{2+} homeostasis, it is essential to determine (a) whether TRPM6 forms functional homomeric channels by itself, and (b) whether TRPM6 channels as well as TRPM6/7 complexes exhibit similar functional characteristics to those of TRPM7.

Mingjiang Li and Jianmin Jiang contributed equally to this work.

Correspondence to Lixia Yue: lyue@uchc.edu

J. Jiang's present address is Department of Pharmacology and Toxicology, Sun Yat-Sen University, People's Republic of China.

The online version of this article contains supplemental material.

Abbreviations used in this paper: 2-APB, 2-aminoethoxydiphenyl borate; DVF, divalent-free solution; HSH, hypomagnesemia and secondary hypocalcemia; MDCT, mouse distal convoluted tubule.

In the present study, we demonstrate that TRPM6, TRPM7, and TRPM6/7 are three distinct ion channels that exhibit different divalent cation permeability, pH sensitivity, and unique single channel conductance. Furthermore, 2-APB differentially regulates channel activities of TRPM6, TRPM7, and TRPM6/7. More importantly, 2-APB markedly increases Mg^{2+} and Ca^{2+} entry through TRPM6. Taken together, our results strongly suggest that TRPM6 forms functional homomeric channels and heteromeric TRPM6/7 channels, and that TRPM6, TRPM7, and TRPM6/7 channels may play different roles under various physiological and/or pathological conditions. Additionally, these findings may prove to be useful tools to distinguish endogenous TRPM6, TRPM7, and TRPM6/7 channels, and perhaps, may provide new insight into channel regulation and information in designing TRPM6 channel activators to facilitate Mg^{2+} absorption.

MATERIALS AND METHODS

Functional Expression of TRPM6, TRPM6^{S141L}, TRPM7, and TRPM6/7

TRPM6 construct was provided by J.G.J. Hoenderop (University Medical Center Nijmegen, Nijmegen, Netherlands). The TRPM6 mutant S141L identified in HSH patients was generated by site-directed mutagenesis (QuickChange, Stratagene) following the standard protocol we previously reported (Yue et al., 2002). The predicted DNA sequence of the mutant was verified by sequencing analysis. TRPM7 was previously cloned from mouse (Runnels et al., 2001).

CHOK1 cells, HEK-293 cells, and MDCT (mouse distal convulsed tube) cells were provided by D.E. Clapham (Harvard Medical School, Boston, MA). Cells were grown in DMEM/F12 medium supplemented with 10% FBS, 100 U/ml penicillin, and 100 mg/ml streptomycin at 37°C in a humidity-controlled incubator with 5% CO_2. Most experiments were conducted in CHOK1 cells (see Discussion) and all the electrophysiological data in the figures are from CHOK1 cells. MDCT cell line was used to study endogenous TRPM6 currents (see Fig. S1, available at http://www.jgp.org/cgi/content/full/jgp.200609502/DC1). CHOK1 or HEK-293 cells were transiently transfected with human TRPM6 wild-type, TRPM6 mutant S141L, TRPM6 plus TRPM7 at 1:1 ratio, or TRPM7 as previously described (Runnels et al., 2001). Electrophysiological recordings were made between 36 and 48 h after transfection. Successfully transfected cells were identified by their green fluorescence when illuminated at 480 nm. Patch-clamp experiments were performed at room temperature (20–25°C).

Electrophysiology

Whole-cell and single-channel currents were recorded using an Axopatch 200B amplifier. Data were digitized at 10 or 20 kHz, and digitally filtered offline at 1 kHz. Patch electrodes were pulled from borosilicate glass and fire polished to a resistance of ~3 MΩ when filled with internal solutions. Series resistance (R_s) was compensated up to 90% to reduce series resistance errors to <5 mV. Cells in which R_s was >10 MΩ were discarded (Yue et al., 2002).

For whole cell current recordings, voltage stimuli lasting 250 ms were delivered at 1–5-s intervals, with either voltage ramps or voltage steps ranging from −120 to +100 mV. Unless otherwise stated, 3–5 min were allowed to let TRPM6 and TRPM7 currents develop and reach a steady state after break-in. A fast perfusion system was used to exchange extracellular solutions. A complete solution exchange was achieved in ~1–3 s.

Single channel currents were recorded in outside-out configuration at various test potentials using patch electrodes with a resistance of ~8–10 MΩ. The pipette solution contained (in mM) 110 $NaSO_3CH_3$, 10 NaCl, 10 HEPES, 10 sodium HEDTA, 2 EGTA pH 7.2. The same solution was used extracellularly in outside-out patches after adding 10 mM glucose.

The internal pipette solution (P1) for whole cell current recordings contained (in mM) 145 Cs-methanesulfonate, 8 NaCl, 10 EGTA, and 10 HEPES, pH adjusted to 7.2 with CsOH. In experiments designed to diminish outward currents, pipette solution (P2) contained (in mM) NMDG 120, glutamic acid 108, HEPES 10, EGTA 10, CsCl 10, pH adjusted to 7.2 with NMDG.

The standard extracellular Tyrode's solution contained (in mM) 140 NaCl, 5 KCl, 2 $CaCl_2$, 20 HEPES, and 10 glucose, pH adjusted to 7.4 (NaOH). External solutions at various acidic pH were prepared as previously reported (Jordt et al., 2000; Askwith et al., 2004; Yermolaieva et al., 2004; Jiang et al., 2005). Divalent-free solution (DVF) contained (in mM) 145 NaCl, 20 HEPES, 5 EGTA, 2 EDTA, and 10 glucose, with estimated free $[Ca^{2+}]$ < 1 nM at pH 7.4 and free $[Mg^{2+}]$ ≈10 nM at pH 7.4 (calculated with the MaxChelator software, available at http://www.stanford.edu/~cpatton/webmaxcS.htm). Isotonic Mg^{2+} and Ca^{2+} and solutions of various divalent cations at different concentrations were prepared as we previously reported (Jiang et al., 2005). 2-aminoethoxydiphenyl borate (2-APB) was dissolved in methanol at 0.5 M stock solution and diluted in extracellular solutions as indicated in the text. All the chemicals were from Sigma-Aldrich.

Quantitative Real-time PCR

Total RNA was extracted from HEK-293 cells transfected with TRPM6, control vector, and TRPM7 using TRIzol reagent (Invitrogen) as previously reported (Yue et al., 1999). RNA was treated with DNase I to prevent contamination of genomic DNA. Total RNA (2 μg) was used in reverse transcription reactions. Quantitative real time PCR (RQ-PCR) was performed using Assays-on-Demand gene expression products from ABI Prism 7500.

Data Analysis

Pooled data are presented as mean ± SEM. Concentration–response curves were fitted by an equation of the form $E = E_{max}\{1/[1 + (EC_{50}/C)^n]\}$, where E is the effect at concentration C, E_{max} is maximal effect, EC_{50} is the concentration for half-maximal effect, and n is the Hill coefficient (Yue et al., 2000). EC_{50} is replaced by IC_{50} if the effect is an inhibitory effect. Statistical comparisons were made using two-way analysis of variance (ANOVA) and two-tailed t test with Bonferroni correction; $P < 0.05$ indicated statistical significance.

Online Supplemental Material

The online supplemental material (Fig. S1, available at http://www.jgp.org/cgi/content/full/jgp.200609502/DC1) elaborates MagNuM/MIC current in MDCT cells.

RESULTS

TRPM6 Expresses Functional Currents in Heterologous Expression System

In CHOK1 cells transiently transfected with TRPM6, outward rectifying currents were elicited by a voltage ramp protocol ranging from −120 to +100 mV (Fig. 1 A). Current amplitude was small immediately after

establishment of the whole-cell configuration, but gradually increased and reached a plateau in ~200 s (Fig. 1 B), presumably due to depletion of intracellular Mg^{2+} (Voets et al., 2004). In the cells transfected with TRPM6 mutant ($TRPM6^{S141L}$) identified in HSH patients, current amplitude was similar as nontransfected cells (Fig. 1 B). Like TRPM7, TRPM6 is permeable to Ca^{2+} and Mg^{2+}, and Ca^{2+} and Mg^{2+} also block monovalent inward currents with an apparent affinity of 5.4 ± 0.3 (n = 6) for Ca^{2+} and 3.4 ± 0.4 μM (n = 8) for Mg^{2+} at −120 mV, similar to those reported by Voets et al. (2004). One of the unique features of TRPM7 is its permeability to a wide array of divalent cations (Monteilh-Zoller et al., 2003). Therefore, we examined whether TRPM6 is also permeable to different divalent cations. The inward current amplitude of different divalent cations was used to represent permeability as previous studies suggested (Nadler et al., 2001; Monteilh-Zoller et al., 2003; Voets et al., 2004). To prevent Na^{+} or other monovalent cations from passing through the channels along with divalent cations, external monovalent cations were replaced by nonpermeant NMDG. Since inward current amplitude is small, we used 30 mM of each divalent cation in order to get bigger inward currents and thereby relatively accurate measurements. However, Zn^{2+} was prepared at 10 mM due to its low solubility at pH 7.4. As shown in Fig. 1 (C and D), TRPM6 inward current was the biggest in 10 mM Zn^{2+}, followed by 30 mM Ba^{2+}, Mg^{2+}, Ca^{2+}, Mn^{2+}, Sr^{2+}, Cd^{2+}, and Ni^{2+}. The ratio of inward current of TRPM6 in 30 mM Ni^{2+} versus Ca^{2+} was 0.52 ± 0.05 (n = 6; Fig. 1 D), ranking Ni^{2+} the least permeant cation to TRPM6. This result is in clear contrast to that of TRPM7, which exhibited high permeability to Ni^{2+} (I_{Ni}/I_{Ca} = 2.3 ± 0.7, n = 7) as shown in Fig. 1

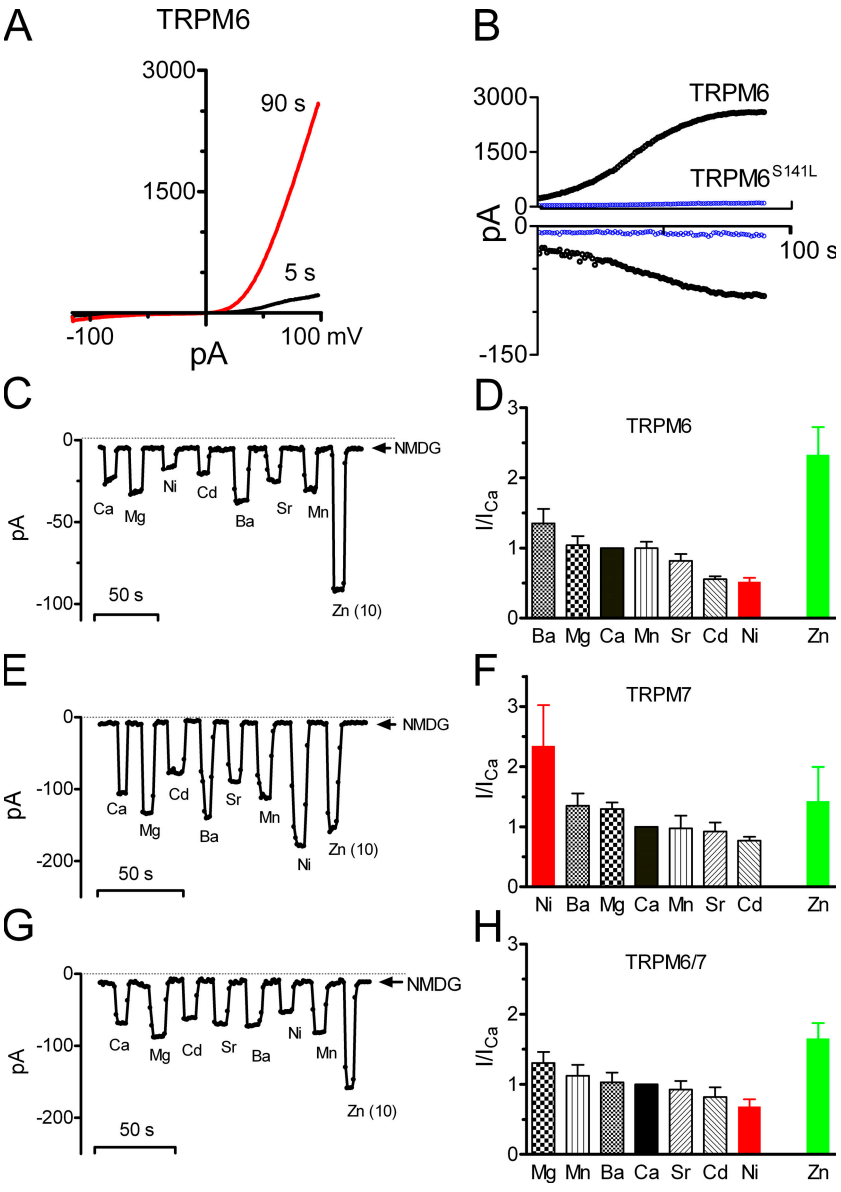

Figure 1. Functional expression of TRPM6 in CHOK1 cells, and relative permeability of TRPM6, TRPM7, and TRPM6/7 to divalent cations. (A) Representative TRPM6 currents elicited by a voltage-ramp ranging from −120 to +100 mV. (B) Changes of current amplitude of wild-type TRPM6 and TRPM6 mutant $TRPM6^{S141L}$ with time. Top, outward current measured at +100 mV; bottom, inward current measured at −120 mV. (C) Inward currents of TRPM6 measured in 30 mM different divalent cation solutions and 10 mM Zn^{2+} solution prepared in nonpermeant NMDG. (D) The ratio of different divalent current amplitude versus Ca^{2+} current amplitude (mean ± SEM, n = 6). (E and G) Inward currents of TRPM7 (E) and TRPM6/7 (G) in the indicated cation solutions. (F and H) The ratio of divalent current amplitude versus Ca^{2+} current amplitude of TRPM7 (F) and TRPM6/7 (H) (mean ± SEM, n = 7).

(E and F) and also as previously reported (Monteilh-Zoller et al., 2003). Except for Ni^{2+}, the relative permeability sequence of other tested cations including Ba^{2+}, Mg^{2+}, Ca^{2+}, Mn^{2+}, Sr^{2+}, and Cd^{2+} of TRPM6 was similar to that of TRPM7. Interestingly, in cells cotransfected with TRPM6 and TRPM7 (TRPM6/7), the permeability sequence was similar but not identical to that of TRPM6 (Fig. 1, G and H), with the largest permeability to Zn^{2+}, and the smallest permeability to Ni^{2+}. In comparison with TRPM7, both TRPM6 and TRPM6/7 exhibited much lower permeability to Ni^{2+}, but much higher permeability to Zn^{2+}. These different permeability profiles suggest that TRPM6, TRPM7, and TRPM6/7 may possess different pore structures.

To test if exogenous overexpression of TRPM6 affected endogenous TRPM7 gene expression, the mRNA level of TRPM7 was examined by quantitative real-time PCR. No difference of endogenous TRPM7 expression was observed in TRPM6- and mock-transfected cells, whereas the mRNA expression of TRPM7 was much higher in the positive control cells, which were transfected with 2 μg TRPM7 (Fig. 2 A). These results indicate that overexpression of TRPM6 did not influence the endogenous expression of TRPM7, suggesting that the currents recorded in TRPM6-transfected cells could not be attributed to up-regulation of endogenous *TRPM7* expression.

We further examined current amplitude in cells transfected with TRPM6 (2 μg), TRPM7 (2 μg), and TRPM6/7 (2 μg in total). The current densities were similar among the three groups, but significantly bigger than that of the endogenous MagNuM/MIC (Fig. 2 B). Similar results were obtained in TRPM6-, TRPM7-, and TRPM6/7-transfected HEK-293 cells (unpublished data). These results suggest that TRPM6 is able to express functional currents without cotransfection with TRPM7.

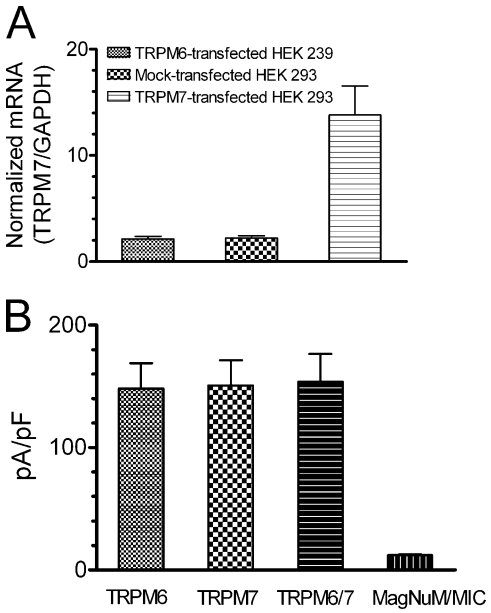

Figure 2. Heterologous overexpression of TRPM6 does not affect endogenous TRPM7 expression. (A) Quantitative real-time PCR results showing similar expression level of endogenous TRPM7 mRNA in TRPM6- and mock-transfected HEK-293 cells. TRPM7-transfected cells were used as a positive control. TRPM7 mRNA was normalized to the internal control GAPDH (mean ± SEM, $n = 5$ for each group). (B) Current density of overexpressed TRPM6 ($n = 17$), TRPM6/7 ($n = 15$) and TRPM7 ($n = 16$) in comparison with that of endogenous MagNuM/MIC ($n = 15$).

Different pH Sensitivity of TRPM6, TRPM7, and TRPM6/7

We have recently reported that TRPM7 inward current is significantly increased by acidic pH (Jiang et al., 2005). As TRPM6 and TRPM7 are closely related homologues, we next examined the effects of low pH on TRPM6 inward currents. As expected, lowering the extracellular pH increased TRPM6 inward currents (Fig. 3, A and B). To compare with the effects of low pH on TRPM7, Fig. 3 (E and F) shows the effects of protons on TRPM7 inward currents. Although the $pH_{1/2}$ was similar between TRPM6 and TRPM7 (Fig. 3 H), the magnitude of increase in TRPM6 inward current (Fig. 3 B) was significantly smaller than that of TRPM7 (Fig. 3 F). For example, pH 4.0 elicited a 9.9 ± 1.3–fold ($n = 6$) (Fig. 3, F and G) increase of TRPM7 inward current, but only a 3.8 ± 0.3–fold ($n = 8$) (Fig. 3, B and G) increase of TRPM6 inward current. In TRPM6/7 coexpressing cells, the increase of inward current was 5.9 ± 0.7–fold ($n = 6$) by pH 4.0 (Fig. 3, C and D, and G). Interestingly, the $pH_{1/2}$ for TRPM6/7 was shifted by one pH unit toward physiological pH 7.4 (Fig. 3 H), indicating an increased sensitivity to acidic pH. At pH 6.0, the increase of TRPM6/7 inward current was much bigger than those of TRPM6 and TRPM7 (Fig. 3 G, right), suggesting that TRPM6/7 channels may play a role under acidic conditions where local pH 6.0 is attained during ischemia and most forms of tissue injury (Reeh and Steen, 1996). As protons potentially compete with divalent cations for binding sites in the external pore of the channels (Jiang et al., 2005), the differences in pH sensitivity further suggest the distinctive pore structures of TRPM6, TRPM7, and TRPM6/7 channels.

Differential Effects of 2-APB on TRPM6, TRPM7, and TRPM6/7

To investigate if there are pharmacological differences, we studied the effects of 2-APB on TRPM6, TRPM7 and TRPM6/7. As shown in Fig. 4 C, 500 μM 2-APB dramatically decreased TRPM7 current amplitude, consistent with the inhibitory effects of 2-APB on endogenous MagNuM/MIC current (Hanano et al., 2004). Surprisingly, TRPM6 current amplitude was significantly increased by the same concentration of 2-APB (Fig. 4 A). Both inward and outward currents of TRPM6 were increased by 2-APB in a concentration-dependent

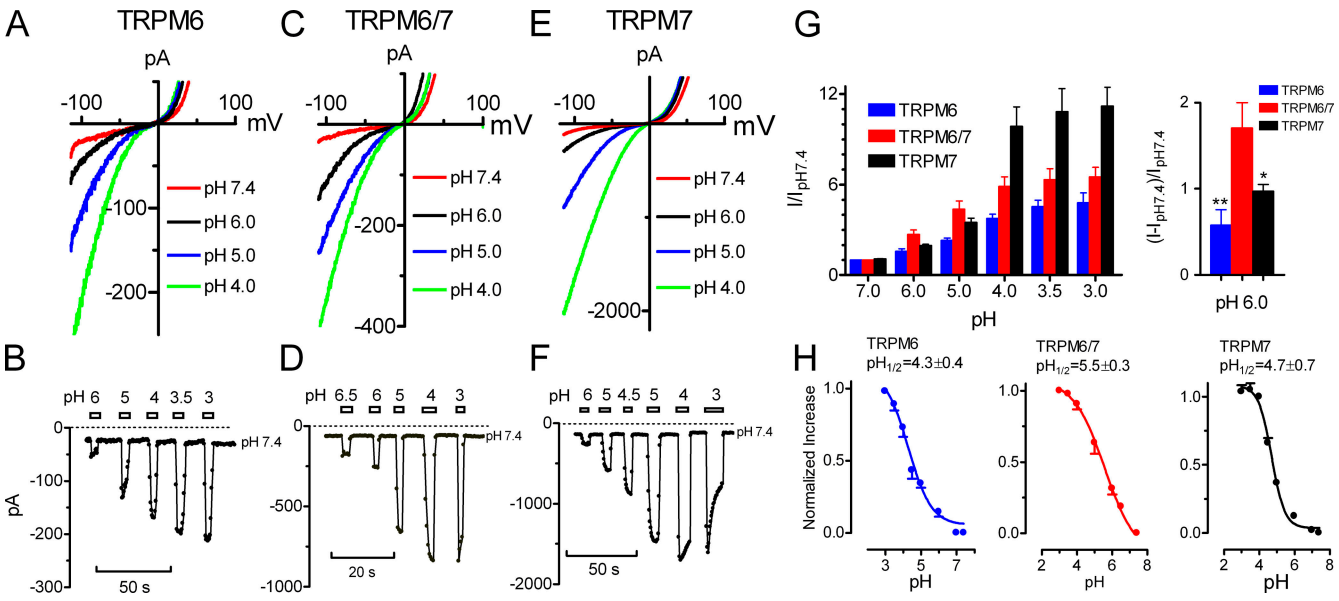

Figure 3. Acidic pH potentiates the inward current of TRPM6, TRPM7, and TRPM6/7. (A, C, and E) Representative recordings of TRPM6 (A), TRPM6/7 (C), and TRPM7 (E) at pH 7.4, 6.0, 5.0, and 4.0, respectively. (B, D, and F) Concentration-dependent changes of inward currents of TRPM6 (B), TRPM6/7 (D), and TRPM7 (F) at the indicated pH values. Note the difference of Y-axis scale of B, D, and F. (G) Averaged inward currents of TRPM6, TRPM7, and TRPM6/7 at the indicated pH values normalized to the value at pH 7.4 (left). The increase of inward current of TRPM6, TRPM7, and TRPM6/7 at pH 6.0 normalized to the value at pH 7.4 (right: *, $P < 0.05$; **, $P < 0.01$). (H) Normalized increase in inward current amplitude and the best-fit of the concentration-dependent curves yielded $pH_{1/2}$ of 4.3 ± 0.4 ($n = 8$, $n_{Hill} = 0.7$) for TRPM6, 4.7 ± 0.7 ($n = 6$, $n_{Hill} = 1.1$) for TRPM7, and 5.5 ± 0.3 ($n = 6$, $n_{Hill} = 0.5$) for TRPM6/7, respectively.

manner (Fig. 4 D), with the EC_{50}s of 380 ± 22 μM (n_{Hill} = 1.8) for the inward currents and 205 ± 10 μM (n_{Hill} = 1.7) (Fig. 4 G) for the outward currents, respectively. We next tested the effects of 2-APB on TRPM6/7 heteromeric channels. As shown in Fig. 4 B, 500 μM 2-APB only slightly increased current amplitude. However, at higher concentrations, 2-APB apparently increased the TRPM6/7 current amplitude (Fig. 4 E). The EC_{50} of 2-APB on TRPM6/7 was 1.6 ± 0.1 mM (n_{Hill} = 1.8) for the outward currents (Fig. 4 G) and 1.7 ± 0.09 mM (n_{Hill} = 1.5) for the inward currents, respectively.

Interestingly, we found that while 2-APB at concentrations <1 mM suppressed TRPM7 currents (Fig. 4, C and F), higher concentrations of 2-APB increased TRPM7 channel activities. Fig. 4 C shows that 2 mM 2-APB apparently potentiated TRPM7 current amplitude. The concentration-dependent increases of TRPM7 inward and outward currents by 2-APB at concentrations >1 mM are shown in Fig. 4 F. At 1.5 mM 2-APB, a transient inhibition was induced before current was increased, followed by a decrease in current amplitude upon washout of 2-APB. The transient inhibition of TRPM7 was smaller at 2, 5, and 10 mM 2-APB. The percentage increase of TRPM7 is shown in Fig. 4 H (top), and the normalized inhibition of TRPM7 at low 2-APB concentrations is shown at the bottom of Fig. 4 H for comparison. The potentiation of 2-APB on TRPM7 did not reach a plateau. However, the effects of 2-APB at >10 mM were not tested due to the solubility limit (Fig. 4 H). The initial transient inhibition as well as the decrease in TRPM7 after washout 2-APB were presumably caused by inhibitory effects of 2-APB at low concentrations, as it is evident that the transient inhibition was smaller at 5 and 10 mM 2-APB.

In summary, at micromolar concentrations, 2-APB enhanced TRPM6 but inhibited TRPM7 currents, whereas at millimolar concentrations, 2-APB increased TRPM7 and TRPM6/7 currents. The differential effects of 2-APB on these channels provide pharmacological evidence that TRPM6, TRPM7, and TRPM6/7 compose distinctive ion channels.

Additive Effects of 2-APB and Protons on TRPM6

Since both protons and 2-APB increase TRPM6 current amplitude, we next examined whether the effects are additive. Fig. 5 shows TRPM6 currents recorded in external solutions at pH 7.4 and pH 5.0, in the presence and absence of 500 μM 2-APB. Changes in TRPM6 inward current amplitude by 2-APB were much bigger at pH 5.0 than that at pH 7.4 (Fig. 5, A and B), suggesting an additive effect between 2-APB and low pH. The additive effects were observed at all the tested pH (Fig. 5 C), although the $pH_{1/2}$ (4.8 ± 0.1, n = 7) was not significantly changed by 2-APB ($pH_{1/2}$ = 4.3 ± 0.4; Fig. 3 H). We also evaluated whether low pH influences the effects of 2-APB on TRPM6. The maximal response induced by

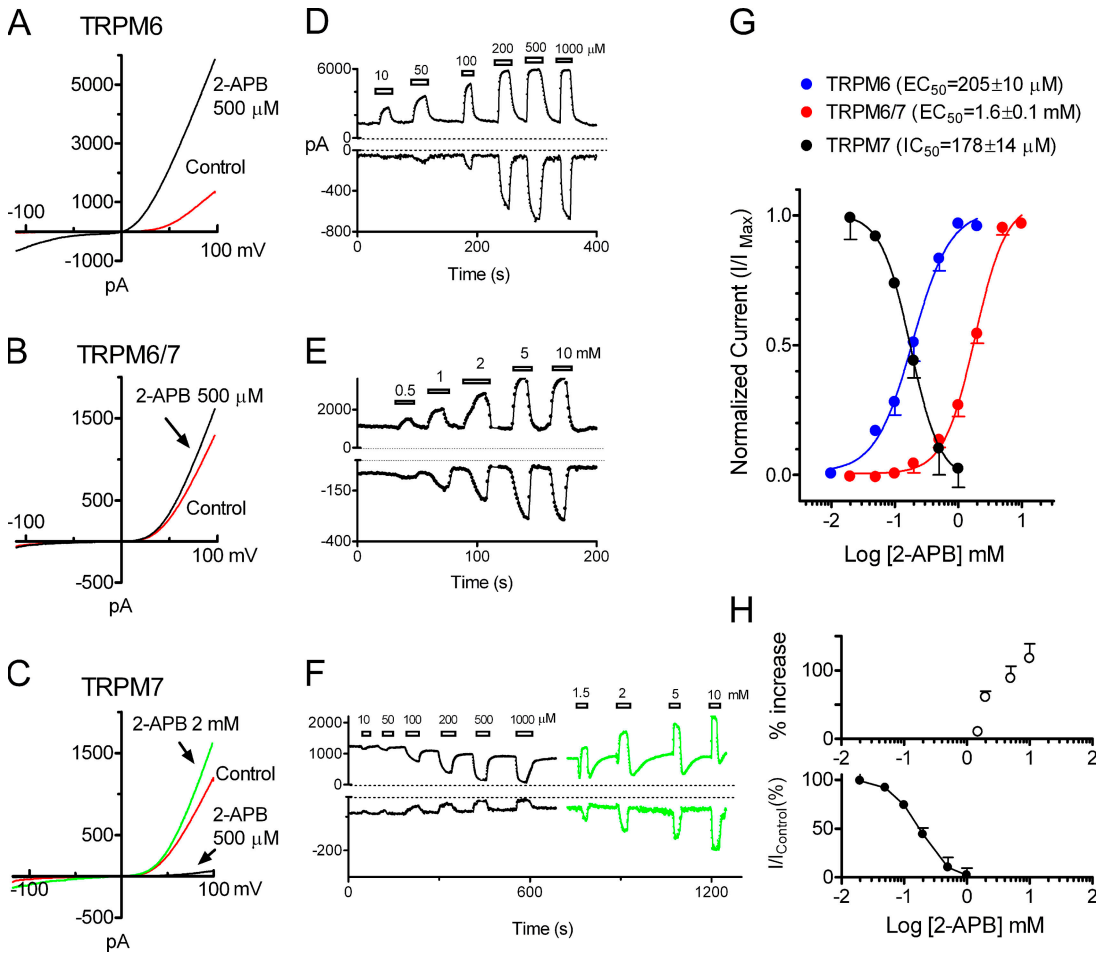

Figure 4. Differential modulation of TRPM6, TRPM7, and TRPM6/7 by 2-APB. (A–C) 500 μM 2-APB significantly increased TRPM6 current (A), markedly inhibited TRPM7 current (C), and moderately enhanced TRPM6/7 current (B). Potentiation of TRPM7 by 2 mM 2-APB is shown in (C). (D–F) Concentration-dependent effects of 2-APB on inward and outward currents of TRPM6 (D), TRPM6/7 (E), and TRPM7 (F). Note the dual-effects of 2-APB on TRPM7. (G) Best-fit of dose–response curves evaluated by using outward currents yielded EC_{50} of 205 ± 10 μM (n_{Hill} = 1.7, n = 7) for TRPM6, IC_{50} of 178 ± 14 μM (n_{Hill} = 1.5, n = 6) for TRPM7, and EC_{50} of 1.6 ± 0.1 mM (n_{Hill} = 1.8, n = 7) for TRPM6/7 complexes. (H). Percentage increase of TRPM7 outward currents by 2-APB at concentrations >1 mM (top, n = 7), and inhibitory effects at low concentrations of 2-APB is shown at the bottom as a comparison.

2-APB at pH 5.0 was similar to that at pH 7.4. However, the EC_{50} of 2-APB (Fig. 5 D) was significantly reduced from 205 ± 10 μM (pH 7.4) to 96.8 ± 13.2 μM (pH 5.0) for outward currents, and from 380 ± 22 μM (pH 7.4) to 92.2 ± 6.8 μM (pH 5.0) for inward current, respectively.

Unique Single Channel Conductance of TRPM6, TRPM7, and TRPM6/7

The above results, including different divalent permeability, pH sensitivity, and distinct effects of 2-APB on TRPM6, TRPM6/7, and TRPM7, suggest that TRPM6, TRPM7, and TRPM6/7 form different ion channels. To further study the pore properties of these channels, we investigated the single channel currents of TRPM6, TRPM7, and TRPM6/7. Whole cell currents in each transfected cell were first confirmed in the Tyrode's solution, and then single channel currents were recorded in DVF under outside-out configuration as previously reported (Yue et al., 2001). Fig. 6 A shows single channel openings in a representative cell transfected with TRPM6. Large current amplitude was observed at negative potentials (Fig. 6 A), with a single channel conductance of 83.6 ± 1.7 pS (Fig. 6 D). Likewise, we measured single channel current of TRPM7 and TRPM6/7 under the same conditions. Single channel current amplitude of TRPM7 was much smaller than that of TRPM6, and the unitary conductance between −120 and −20 mV was 40.1 ± 1.0 pS (Fig. 6, C and D). Furthermore, when TRPM6 and TRPM7 were coexpressed, a novel single channel conductance of 56.6 ± 3.7 pS was produced, indicating that TRPM6 and TRPM7 can form heterotetrameric ion channels. These different single channel conductances indicate that TRPM6, TRPM7, and TRPM6/7 channels have distinct pore structures.

In TRPM6 and TRPM7 cotransfected cells, TRPM6 and TRPM7 may randomly form heterotetrameric

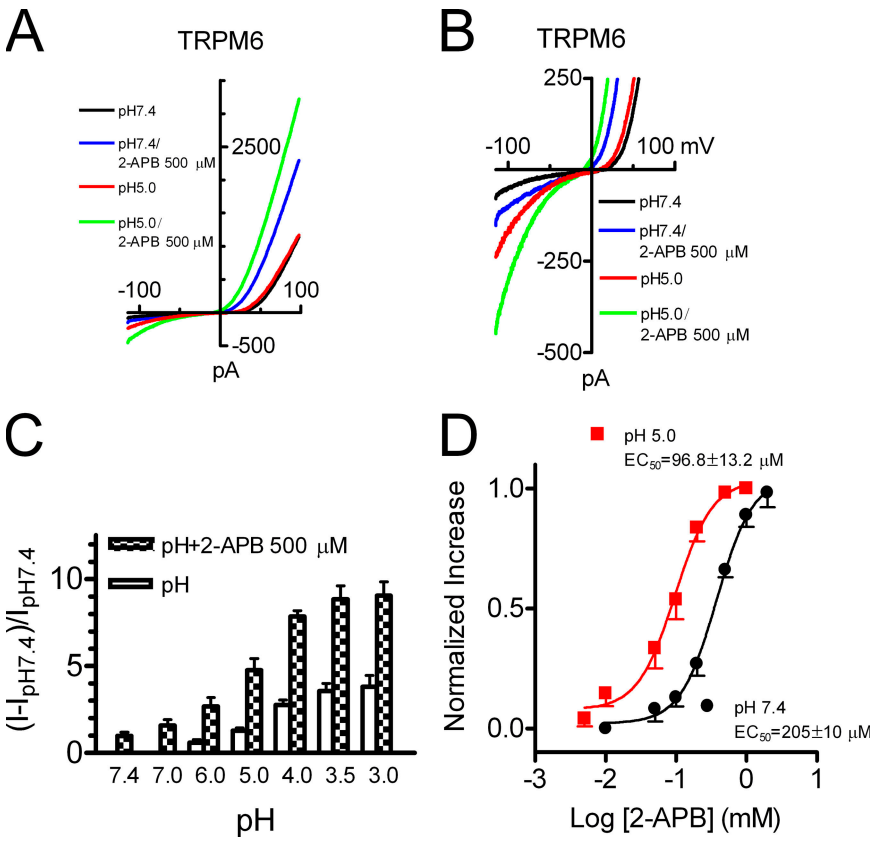

Figure 5. Additive effects of 2-APB and acidic pH on TRPM6. (A and B) Effects of 500 μM 2-APB on TRPM6 at pH 7.4 and pH 5.0. Changes in inward current are shown in B with expanded Y-axis scale. (C) Effects of acidic pH on TRPM6 inward current in the presence and absence of 500 μM 2-APB. (D) Acidic pH enhanced the effects of 2-APB on TRPM6. The EC_{50} of 2-APB evaluated using outward current was significantly decreased from EC_{50} = 205 ± 10 μM (n = 7, n_{Hill} = 1.7) at pH 7.4 to EC_{50} = 96.8 ± 13.2 μM (n = 8, n_{Hill} = 1.6) at pH 5.0.

channels with different configurations. Indeed, in the patches that contain two or more channels, single channels with different current amplitudes were observed (Fig. 7 C). All points histogram (Fig. 7 D) illustrates the single channel current amplitudes corresponding to the single channel conductances of TRPM6, TRPM7, and TRPM6/7, suggesting the existence of both heterotetrameric TRPM6/7 channels and homotetrameric TRPM6 and TRPM7 channels in the TRPM6/7 coexpressing cells. In another three separated patches that contain three channels, similar histograms corresponding to the unitary conductances of 83.6, 56.6, and 40.1 pS were obtained, suggesting that the heterotetramers with unitary conductance of 56.6 is the preferred configuration when TRPM6 and TRPM7 are expressed at a 1:1 ratio. In comparison with the TRPM6/7 coexpressing cells, only one type of single channel was observed in TRPM6- or TRPM7-transfected cells (Fig. 7, A and B, E and F).

Increased Mg^{2+} and Ca^{2+} Permeability of TRPM6

Both TRPM6 and TRPM7 are important in Mg^{2+} homeostasis. Dysfunction of TRPM6 results in HSH (Schlingmann et al., 2002, 2005; Walder et al., 2002), whereas deletion of TRPM7 causes Mg^{2+} deficiency, thereby leading to cell death (Schmitz et al., 2003, 2005). Since 2-APB significantly increased TRPM6 inward currents, we next investigated whether Mg^{2+} and Ca^{2+} currents are increased by 2-APB. Fig. 8 shows that the inward Ca^{2+} and Mg^{2+} currents of TRPM6 recorded in isotonic Ca^{2+} and Mg^{2+} solutions were significantly enhanced by 2-APB. The reversal potentials were also shifted toward more positive direction, consistent with the increased inward currents. These results imply that Mg^{2+} and Ca^{2+} entry through TRPM6 can be pharmacologically potentiated.

DISCUSSION

In the present study, we have demonstrated several unique functional characteristics of TRPM6, which distinguish TRPM6 from those of TRPM7 and TRPM6/7 channels. Our findings indicate that TRPM6 forms functional homomeric channels on its own and heteromeric channels in combination with TRPM7. Moreover, we found that TRPM6 channel activity, as well as Mg^{2+} and Ca^{2+} entry through TRPM6, can be significantly potentiated.

TRPM6, TRPM7, and TRPM6/7 compose distinct ion channels

TRPM6 and TRPM7 are two unique channel kinases. Although the kinase function is not fully understood (Nadler et al., 2001; Runnels et al., 2001; Ryazanova et al., 2004; Matsushita et al., 2005), the channel function in permeating Mg^{2+} seems essential for cell viability (Nadler et al., 2001; Schmitz et al., 2003; Schmitz et al., 2005) and Mg^{2+} homeostasis in humans

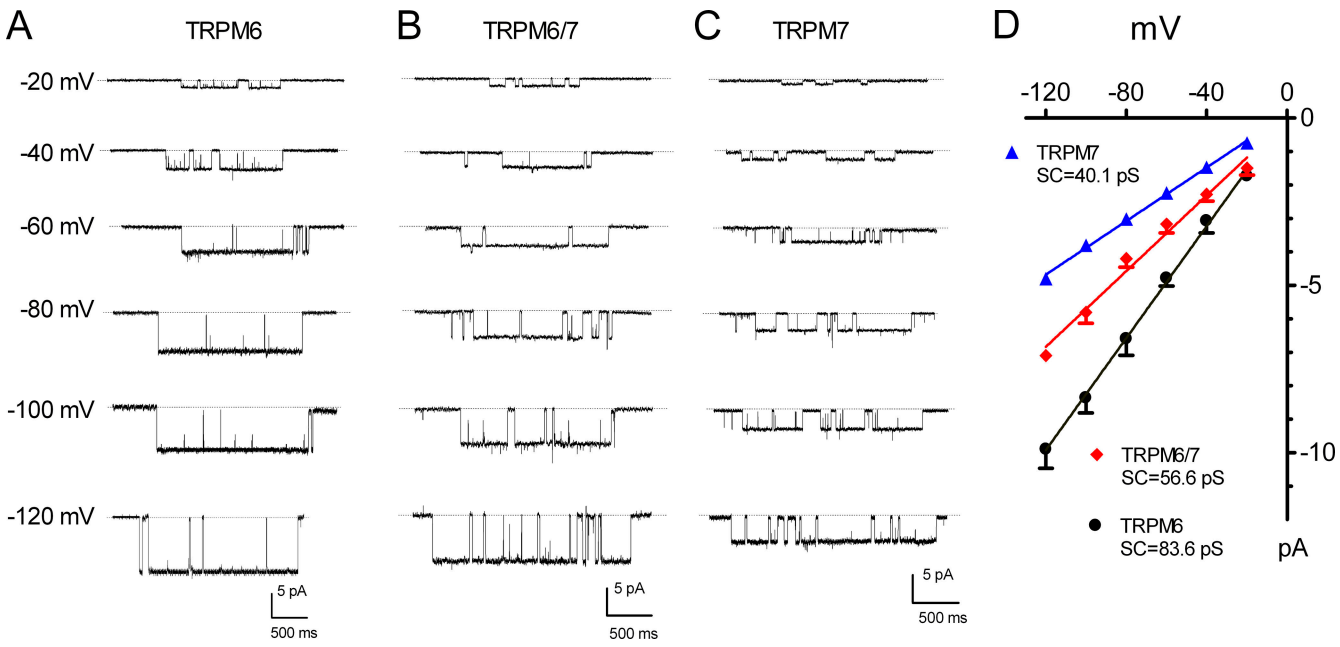

Figure 6. Unique single channel conductance of TRPM6, TRPM7, and TRPM6/7. (A–C) Representative recordings of TRPM6, TRPM6/7, and TRPM7 at various voltages in outside-out configuration. Dashed lines represent zero current level. (D) Averaged current amplitude of TRPM6, TRPM7, and TRPM6/7 plotted as a function of test potentials. Linear regression fit of the mean current amplitude produced the unitary conductance of 83.6 ± 1.7 (n = 8), 56.6 ± 3.7 (n = 6), and 40.1 ± 1.0 pS (n = 8) for TRPM6, TRPM6/7, and TRPM7, respectively.

(Schlingmann et al., 2002; Walder et al., 2002; Schlingmann and Gudermann, 2005; Schlingmann et al., 2005). Functional characteristics of TRPM7 have been well studied (Nadler et al., 2001; Runnels et al., 2001, 2002; Aarts et al., 2003; Kerschbaum et al., 2003; Monteilh-Zoller et al., 2003; Hanano et al., 2004; Takezawa et al., 2004; Elizondo et al., 2005; Kozak et al., 2005), whereas conflicting findings in terms of whether TRPM6 forms functional channels have been reported (Chubanov et al., 2004; Voets et al., 2004). In the present study, although we do not have explanations for the different findings (Chubanov et al., 2004; Voets et al., 2004), we provide several lines of evidence demonstrating that TRPM6, TRPM7, and TRPM6/7 channels are biophysically and pharmacologically distinguishable, and that TRPM6, TRPM7, and TRPM6/7 form distinct ion channels.

First, TRPM6, TRPM7, and TRPM6/7 display different divalent cation permeability profiles. Although TRPM6 (Voets et al., 2004), TRPM7 (Nadler et al., 2001; Runnels et al., 2001), and TRPM6/7 (Chubanov et al., 2004) in heterologous expression systems produce identical outward rectifying I-V curves (Fig. 1 A and Fig. 4, A–C), and exhibit similar permeation to Ca^{2+} and Mg^{2+} and other divalent cations, we found that the relative permeability to Ni^{2+} is significantly different among these three different types of channels (Fig. 1). As the pore structure of a channel plays a crucial role in determining its ionic permeability and selectivity properties (Hille, 2003; Owsianik et al., 2005), the different ionic permeation profiles suggest that TRPM6, TRPM7, and TRPM6/7 channels comprise distinct channel pores.

Second, TRPM6, TRPM7, and TRPM6/7 exhibit different sensitivity to low pH. We previously demonstrated that external protons compete with divalent cations for the binding sites in the putative channel pore of TRPM7 (Jiang et al., 2005). Between transmembrane domains 5 and 6, there are seven negatively charged residues for TRPM7 and eight negatively charged residues for TRPM6. These differences in the pore structure may explain the increased sensitivity of TRPM6/7 to low pH and the varied degree of potentiation in inward currents of TRPM6, TRPM7, and TRPM6/7 elicited by low pH (Fig. 3).

Third, the most striking biophysical difference among TRPM6, TRPM7, and TRPM6/7 is their unique single channel conductance. The unitary conductance of TRPM6 (83.6 pS) is much bigger than that of TRPM7 (40.1 pS), although they share ~80% sequence identity in the putative pore region. When TRPM6 and TRPM7 form heterotetramers, a novel conductance (56.6 pS) is produced. As the single channel conductance is a signature feature of an ion channel, these differences in single channel conductance (Fig. 6) strongly suggest that TRPM6 forms homomeric channels as well as TRPM6/7 heteromeric channels.

The new conductance obtained in TRPM6/7 coexpressing cells indicates that TRPM6 and TRPM7 indeed

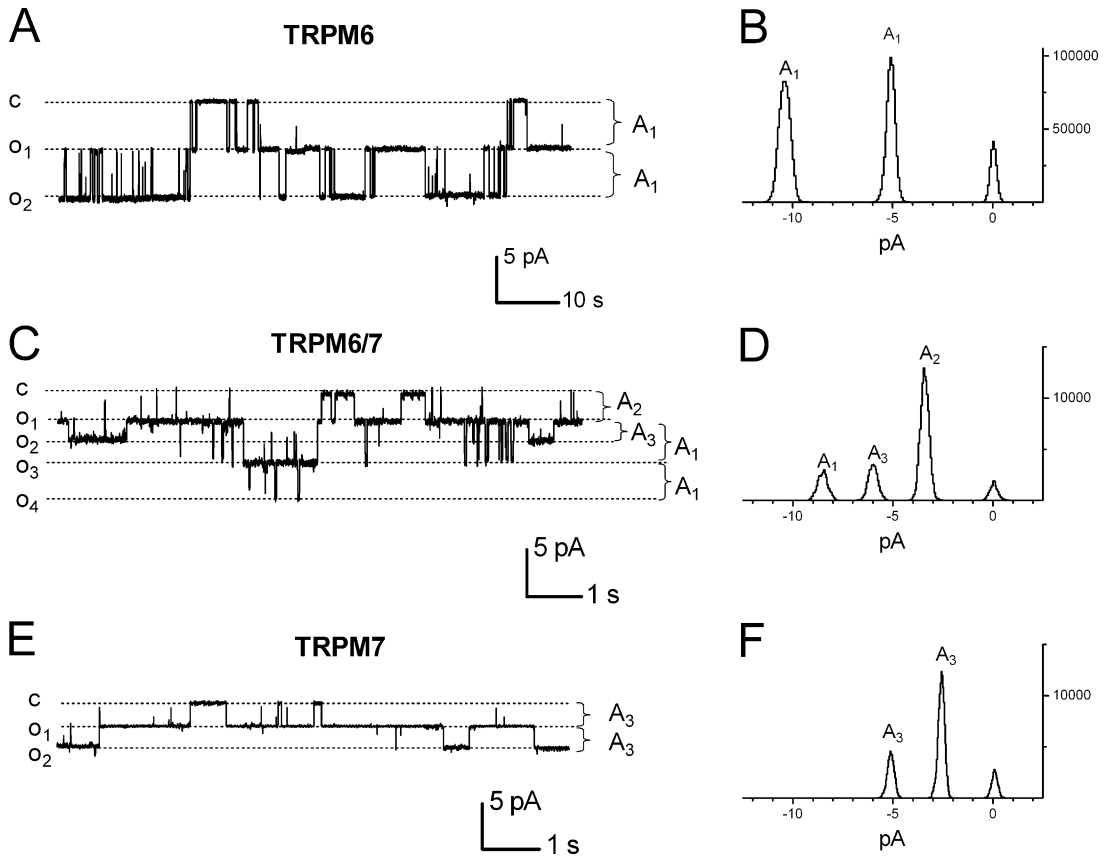

Figure 7. Histogram of single channel currents in TRPM6, TRPM6/7 (1:1 ratio), and TRPM7-expressing cells. (A, C, and E) Representative recordings of single channel opening at −60 mV from different cells. Two or three channels were observed in each patch. Dashed lines represent different closing or opening states of single channels. "C" represents closing state; "O1," "O2," "O3," and "O4" represent different opening states; and "A1", "A2," and "A3" represent different current amplitudes. (B, D, and F) All point histogram of single channel current amplitudes obtained under each condition as shown in A, C, and E. Current amplitudes A1, A2, and A3 represent the amplitudes corresponding to the unitary conductances of 83.6 pS (TRPM6), 56.6 pS (TRPM6/7), and 40.1 pS (TRPM7), respectively. Note that there were three different conductances in TRPM6/7-expressing cells (C and D), whereas only one conductance was observed in TRPM6 (A and B) or TRPM7 (E and F) expressing cells. Similar results were observed in another three separated patches for each group ($n = 4$ for each group).

form functional heteromeric channels. This result is consistent with previous findings that TRPM6 and TRPM7 physically interact (Chubanov et al., 2004; Schmitz et al., 2005). It is interesting that an intermediate single channel conductance (56.6 pS) was obtained for TRPM6/7 heteromeric channels. Heteromultimerization has been reported to occur within other highly homologous TRP channels, such as TRPC1/4/5 (Strubing et al., 2001, 2003), TRP1/3 (Lintschinger et al., 2000), TRPC3/6/7 (Vennekens et al., 2002), and TRPV5/6. The single channel conductance of TRPC1/5 multimers is much smaller than that of TRPC5 homomers (Strubing et al., 2001). TRPV5/6 complex exhibits many properties intermediate to those of TRPV5 and TRPV6, yet the single channel conductance of TRPV5/6 heterotetramer was not determined (Hoenderop et al., 2003). Durkun and colleagues demonstrated that hybrid gramicidin channels of [Gly^1]gramicidin C and [Val^1]gramicidin produce single channel conductances that are intermediate to those of the corresponding symmetric channels (Durkin et al., 1990), whereas heterodimers of des-Val^1-[Ala^2]gA and [Val^1]gA resulted in single channel conductances that are smaller than either of the symmetric channel types (Durkin et al., 1993). The intermediate single channel conductances have been observed for heteromeric K^+ channels. When the WT and T442S mutant of *Shaker* potassium channel subunit form heteromultimers, four new intermediate single channel conductances are observed besides the two conductances of homomultimeric channels (Zheng and Sigworth, 1998). Intermediate single channel conductances were also reported in heterotetrameric Kir 1.1 channels (Wang et al., 2005). Coexpression of CNG channel subunits RET and RO133 yields four classes of intermediate conductance (Liu et al., 1996, 1998). Therefore, generation of intermediate single channel conductances is a common phenomenon observed in heteromultimer channels.

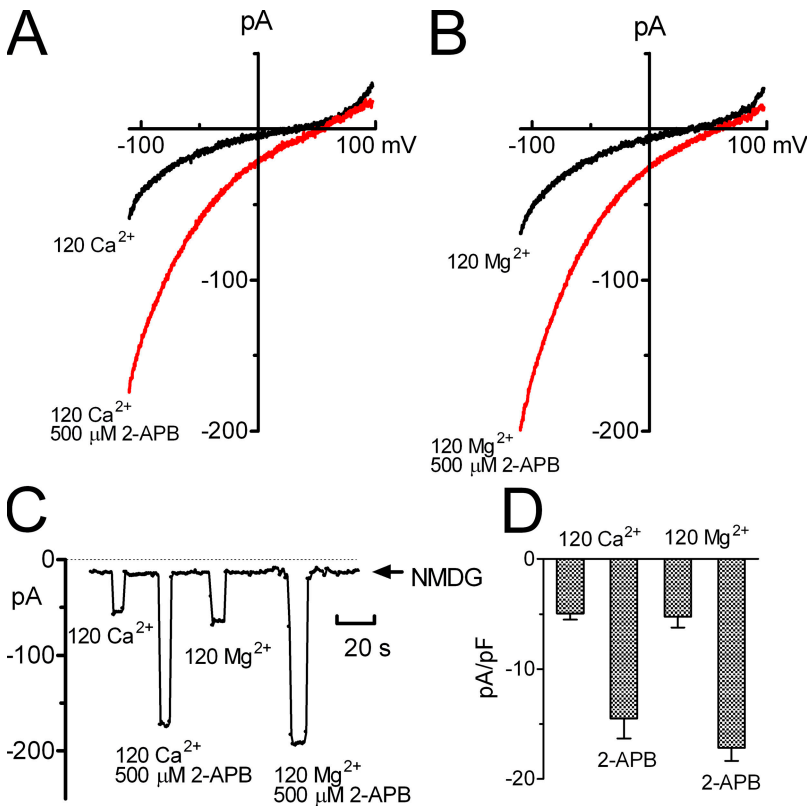

Figure 8. Increased Mg^{2+} and Ca^{2+} permeability of TRPM6. (A and B) Effects of 2-APB on TRPM6 currents recorded in isotonic 120 Ca^{2+} and 120 Mg^{2+} solutions (in mM) with P2 pipette solution. (C) Inward currents measured at −120 mV plotted against time. (D) Average inward current density of TRPM6 under the indicated conditions ($n = 8$).

We observed one intermediate single channel conductance (56.6 pS) by coexpressing of TRPM6/7 plasmids at 1:1 ratio. This conductance might represent the heterotetrameric channels that compose two TRPM6 and two TRPM7 subunits. It is possible that other intermediate conductances can be produced when heterotetramers are formed at 3:1 or 1:3 ratios of TRPM6 and TRPM7. Further experiments are required to address this question.

Fourth, TRPM6, TRPM7, and TRPM6/7 channels are differentially regulated by 2-APB. The detailed mechanism by which 2-APB modulates TRPM6, TRPM7, and TRPM6/7 requires further investigation. However, it is apparent that the mechanism of 2-APB's effects is different from that of protons, because the effects of 2-APB and protons on TRPM6 are additive (Fig. 5). The different responses to 500 μM 2-APB among TRPM6, TRPM7, and TRPM6/7 are so striking that TRPM6, TRPM7, and TRPM6/7 currents can be differentiated by 500 μM 2-APB. Therefore, the effect of 2-APB represents an independent line of evidence indicating that TRPM6, TRPM7, and TRPM6/7 form three distinct types of ion channels.

2-APB was initially found to inhibit IP_3 receptor, thereby suppressing intracellular Ca^{2+} release (Maruyama et al., 1997; Wu et al., 2000). Recent studies have demonstrated that this compound exhibits effects on I_{CRAC} (Prakriya and Lewis, 2001; Bootman et al., 2002), TRP channels (Voets et al., 2001; Chung et al., 2004, 2005; Hu et al., 2004; Wicher et al., 2005; Xu et al., 2005), SERCA Ca^{2+} pumps (Bilmen et al., 2002), endogenous nonselective cation current (Braun et al., 2003), and anion channels (Lemonnier et al., 2004). The clearly opposite effects of 2-APB at micromolar concentrations on TRPM6 and TRPM7 is intriguing, as TRPM6 and TRPM7 share 50–80% similarities. It is also interesting that 2-APB produces dual-effects on TRPM7 (Fig. 4 F) but not on TRPM6 (not depicted) or TRPM6/7 (Fig. 4 E). The concentration window of 2-APB for inhibiting and activating of TRPM7 is very narrow. A similar dual-effect of 2-APB on I_{CRAC} has been previously reported (Prakriya and Lewis, 2001). Prakriya and Lewis found that 5 μM 2-APB significantly increases I_{CRAC}, whereas 10 μM 2-APB initially potentiates I_{CRAC} and then irreversibly inhibits I_{CRAC}. The mechanism of the dual-effect of 2-APB is unknown, yet it is possible that 2-APB binds to different sites of the channel protein, therefore producing opposite effects on TRPM7. Although 2-APB may not produce physiological and/or pathological impact due to the high concentrations required, it is a useful tool to differentiate TRPM6, TRPM7, and TRPM6/7. Indeed, in an attempt to record endogenous TRPM6 currents in MDCT cell line, we found that MagNuM/MIC currents in MDCT cells were inhibited by 500 μM 2-APB but potentiated by 2 mM 2-APB (see Fig. S1, available at http://www.jgp.org/cgi/content/full/jgp.200609502), suggesting that TRPM6 currents and TRPM6/7 currents are unlikely

present in MDCT cell line under our experimental conditions. Therefore, although TRPM6 has been found to be highly expressed in the native distal convoluted tubule (DCT) (Voets et al., 2004), the DCT cell line derived from mouse may not be a good model system to study TRPM6. More detailed studies are required in order to understand the underlying mechanisms by which 2-APB activates TRPM6 and inhibits TRPM7 at low concentrations, as well as activates TRPM7 at high concentrations.

Potential Significance

The present study provides strong evidence indicating that the channel kinase, TRPM6, whose mutations cause HSH (Schlingmann et al., 2002, 2005; Walder et al., 2002), forms functional homomeric channels by itself and heteromeric channels with TRPM7. Understanding the unique functional characteristics of TRPM6 will extend our understanding of potential roles and regulatory mechanisms of TRPM6 in HSH.

The unique properties of TRPM6 discovered in the present study, including the unique single channel conductance, activation by 2-APB, and sensitivity to low pH, may serve as functional identifications of TRPM6, which could be used as potential tools to distinguish TRPM6 from TRPM7 and TRPM6/7 channels. TRPM6 and TRPM7 share 50% sequence identity and are the closest homologues in the TRPM subfamily. There were no available tools to differentiate TRPM6 and TRPM7 channels because the known properties (Voets et al., 2004), such as outward rectifying I-V curve, intracellular Mg^{2+} regulation, and external Ca^{2+} and Mg^{2+} block of the two channels, are similar. We have shown in the present study that TRPM6, TRPM7, and TRPM6/7 channel activities are differentially regulated by 2-APB. While TRPM6 is maximally increased by 500 μM 2-APB, TRPM7 is largely inhibited by the same concentration of 2-APB but significantly activated by 2 mM 2-APB; TRPM6/7 is slightly increased by 500 μM 2-APB but significantly increased by 2 mM 2-APB. Although 2-APB also increases TRPV1, TRPV2, TRPV3 (Chung et al., 2004; Hu et al., 2004), and TRPV6 (Voets et al., 2001) and inhibits TRPC5 (Xu et al., 2005), TRPC6, and TRPM8 (Chung et al., 2004; Hu et al., 2004), the unique responses of TRPM6, TRPM7, and TRPM6/7 to 2-APB, in conjugation with other features of TRPM6 and TRPM7, such as different sensitivity to pH and unique single channel conductances, should prove to be useful in distinguishing endogenous TRPM6, TRPM7, and TRPM6/7 currents.

The increased channel activity of TRPM6 and TRPM6/7 by 2-APB provides the first evidence that these Mg^{2+}-permeable channels can be pharmacologically activated. Moreover, both Mg^{2+} and Ca^{2+} currents through TRPM6 were increased (Fig. 8), implying that it is possible to increase Mg^{2+} and Ca^{2+} absorption by regulating TRPM6 and TRPM6/7 channel activities. Given the potential importance of TRPM6 and TRPM7 in Mg^{2+} homeostasis (Nadler et al., 2001; Schlingmann et al., 2002; Walder et al., 2002; Schmitz et al., 2003, 2005; Schlingmann and Gudermann, 2005; Schlingmann et al., 2005; Schmitz et al., 2005), our findings that channel activity and Mg^{2+} entry of TRPM6 and TRPM6/7 can be increased by 2-APB may provide an important clue as to searching or designing channel activators to increase Mg^{2+} entry.

Potential Limitations

Our data indicate that TRPM6 forms functional homomeric channels by itself, as well as heteromeric channels in combination with TRPM7. Since all the experiments were performed in CHOK1 cells that contain endogenous TRPM7, we cannot exclude the possibility that endogenous TRPM7 may have played a role in functional expression of TRPM6. However, given that the endogenous TRPM7 current amplitude of CHOK1 cells is only 1/10 that of the TRPM6 current amplitude, the predominant channel form (90%) should be homomeric TRPM6 channels when TRPM6 is overexpressed in CHOK1 cells. In addition, we also transfected TRPM6 to HEK-293 cells, which have larger endogenous TRPM7 currents than CHOK1 cells. No differences in current amplitude and 2-APB response were observed between TRPM6 expressed in CHOK1 cells and HEK-293 cells (unpublished data). Nonetheless, the dramatic differences in single channel conductance, 2-APB response, divalent cation permeability, and pH sensitivity indicate that TRPM6, TRPM7, and TRPM6/7 are three distinct types of channels. Future studies using cells from TRPM7 knockout animals will help to clarify whether TRPM6 can form the same functional channels in the absence of TRPM7.

In TRPM6/7 coexpression experiment, we used 1:1 ratio of TRPM6 and TRPM7 cDNA for transfection. However, it is difficult to know whether the TRPM6/7 complexes have 1:1 ratio of TRPM6 and TRPM7 subunits. Investigating single channel properties and whole-cell TRPM6/7 current characteristics by coexpressing TRPM6 and TRPM7 at various ratios, or by making concatemeric channels as previous reported (Hoenderop et al., 2003), will answer if the biophysical and pharmacological properties of TRPM6/7 complexes are different when the complexes contain different compositions of TRPM6 and TRPM7 subunits. This will provide insight into subunit stoichiometry of TRPM6/7 heteromers in heterologous expression systems and shed light on endogenous TRPM6/7 complex configurations.

In conclusion, we demonstrated that TRPM6, TRPM7, and TRPM6/7 represent three different types of channels with unique functional characteristics. Our data indicate that both TRPM6 and TRPM7 are able to form homotetrameric as well as heterotretrameric channels. The distinct characteristics of TRPM6, TRPM7, and

TRPM6/7 suggest that they may play different roles under physiological and/or pathological conditions. The increased channel activity of TRPM6 and TRPM6/7 by 2-APB and increased Mg^{2+} entry through TRPM6 may provide new insight into channel regulation and information in designing channel activators to facilitate Mg^{2+} absorption.

We thank Dr. Joost G.J. Hoenderop for providing TRPM6 in the pCINeo/IRES-GFP vector; Drs. Alan Fein, David Clapham, Bruce Liang, Kimberly Dodge, Laurinda Jaffe, Haoxing Xu, and Dejian Ren for their constructive suggestions and comments.

This work was supported by American Heart Association grant (0335124N), and by a National Institutes of Health grant (HL078960) to L. Yue.

David C. Gadsby served as editor.

Submitted: 31 January 2006
Accepted: 30 March 2006

REFERENCES

Aarts, M., K. Iihara, W.L. Wei, Z.G. Xiong, M. Arundine, W. Cerwinski, J.F. MacDonald, and M. Tymianski. 2003. A key role for TRPM7 channels in anoxic neuronal death. *Cell.* 115:863–877.

Askwith, C.C., J.A. Wemmie, M.P. Price, T. Rokhlina, and M.J. Welsh. 2004. Acid-sensing ion channel 2 (ASIC2) modulates ASIC1 H^+-activated currents in hippocampal neurons. *J. Biol. Chem.* 279:18296–18305.

Bilmen, J.G., L.L. Wootton, R.E. Godfrey, O.S. Smart, and F. Michelangeli. 2002. Inhibition of SERCA Ca^{2+} pumps by 2-aminoethoxydiphenyl borate (2-APB). 2-APB reduces both Ca^{2+} binding and phosphoryl transfer from ATP, by interfering with the pathway leading to the Ca^{2+}-binding sites. *Eur. J. Biochem.* 269:3678–3687.

Bootman, M.D., T.J. Collins, L. Mackenzie, H.L. Roderick, M.J. Berridge, and C.M. Peppiatt. 2002. 2-aminoethoxydiphenyl borate (2-APB) is a reliable blocker of store-operated Ca^{2+} entry but an inconsistent inhibitor of InsP3-induced Ca^{2+} release. *FASEB J.* 16:1145–1150.

Braun, F.J., O. Aziz, and J.W. Putney Jr. 2003. 2-aminoethoxydiphenyl borane activates a novel calcium-permeable cation channel. *Mol. Pharmacol.* 63:1304–1311.

Chubanov, V., S. Waldegger, M. Mederos y Schnitzler, H. Vitzthum, M.C. Sassen, H.W. Seyberth, M. Konrad, and T. Gudermann. 2004. Disruption of TRPM6/TRPM7 complex formation by a mutation in the TRPM6 gene causes hypomagnesemia with secondary hypocalcemia. *Proc. Natl. Acad. Sci. USA.* 101:2894–2899.

Chubanov, V., Y.S.M. Mederos, J. Waring, A. Plank, and T. Gudermann. 2005. Emerging roles of TRPM6/TRPM7 channel kinase signal transduction complexes. *Naunyn Schmiedebergs Arch. Pharmacol.* 371:334–341.

Chung, M.K., H. Lee, A. Mizuno, M. Suzuki, and M.J. Caterina. 2004. 2-aminoethoxydiphenyl borate activates and sensitizes the heat-gated ion channel TRPV3. *J. Neurosci.* 24:5177–5182.

Chung, M.K., A.D. Guler, and M.J. Caterina. 2005. Biphasic currents evoked by chemical or thermal activation of the heat-gated ion channel, TRPV3. *J. Biol. Chem.* 280:15928–15941.

Clapham, D.E. 2003. TRP channels as cellular sensors. *Nature.* 426:517–524.

Durkin, J.T., R.E. Koeppe II, and O.S. Andersen. 1990. Energetics of gramicidin hybrid channel formation as a test for structural equivalence. Side-chain substitutions in the native sequence. *J. Mol. Biol.* 211:221–234.

Durkin, J.T., L.L. Providence, R.E. Koeppe II, and O.S. Andersen. 1993. Energetics of heterodimer formation among gramicidin analogues with an NH_2-terminal addition or deletion. Consequences of missing a residue at the join in the channel. *J. Mol. Biol.* 231:1102–1121.

Elizondo, M.R., B.L. Arduini, J. Paulsen, E.L. MacDonald, J.L. Sabel, P.D. Henion, R.A. Cornell, and D.M. Parichy. 2005. Defective skeletogenesis with kidney stone formation in dwarf zebrafish mutant for trpm7. *Curr. Biol.* 15:667–671.

Fleig, A., and R. Penner. 2004. Emerging roles of TRPM channels. *Novartis Found. Symp.* 258:248–258.

Hanano, T., Y. Hara, J. Shi, H. Morita, C. Umebayashi, E. Mori, H. Sumimoto, Y. Ito, Y. Mori, and R. Inoue. 2004. Involvement of TRPM7 in cell growth as a spontaneously activated Ca^{2+} entry pathway in human retinoblastoma cells. *J. Pharmacol. Sci.* 95:403–419.

Harteneck, C., T.D. Plant, and G. Schultz. 2000. From worm to man: three subfamilies of TRP channels. *Trends Neurosci.* 23:159–166.

Hermosura, M.C., H. Nayakanti, M.V. Dorovkov, F.R. Calderon, A.G. Ryazanov, D.S. Haymer, and R.M. Garruto. 2005. A TRPM7 variant shows altered sensitivity to magnesium that may contribute to the pathogenesis of two Guamanian neurodegenerative disorders. *Proc. Natl. Acad. Sci. USA.* 102:11510–11515.

Hille, B. 2003. Ion Channels of Excitable Membranes. Third edition. Sinauer Associates, Inc. Sunderland, MA. 471–502.

Hoenderop, J.G., T. Voets, S. Hoefs, F. Weidema, J. Prenen, B. Nilius, and R.J. Bindels. 2003. Homo- and heterotetrameric architecture of the epithelial Ca^{2+} channels TRPV5 and TRPV6. *EMBO J.* 22:776–785.

Hu, H.Z., Q. Gu, C. Wang, C.K. Colton, J. Tang, M. Kinoshita-Kawada, L.Y. Lee, J.D. Wood, and M.X. Zhu. 2004. 2-aminoethoxydiphenyl borate is a common activator of TRPV1, TRPV2, and TRPV3. *J. Biol. Chem.* 279:35741–35748.

Jiang, J., M. Li, and L. Yue. 2005. Potentiation of TRPM7 inward currents by protons. *J. Gen. Physiol.* 126:137–150.

Jordt, S.E., M. Tominaga, and D. Julius. 2000. Acid potentiation of the capsaicin receptor determined by a key extracellular site. *Proc. Natl. Acad. Sci. USA.* 97:8134–8139.

Kerschbaum, H.H., J.A. Kozak, and M.D. Cahalan. 2003. Polyvalent cations as permeant probes of MIC and TRPM7 pores. *Biophys. J.* 84:2293–2305.

Kozak, J.A., M. Matsushita, A.C. Nairn, and M.D. Cahalan. 2005. Charge screening by internal pH and polyvalent cations as a mechanism for activation, inhibition, and rundown of TRPM7/MIC channels. *J. Gen. Physiol.* 126:499–514.

Lemonnier, L., N. Prevarskaya, J. Mazurier, Y. Shuba, and R. Skryma. 2004. 2-APB inhibits volume-regulated anion channels independently from intracellular calcium signaling modulation. *FEBS Lett.* 556:121–126.

Lintschinger, B., M. Balzer-Geldsetzer, T. Baskaran, W.F. Graier, C. Romanin, M.X. Zhu, and K. Groschner. 2000. Coassembly of Trp1 and Trp3 proteins generates diacylglycerol- and Ca^{2+}-sensitive cation channels. *J. Biol. Chem.* 275:27799–27805.

Liu, D.T., G.R. Tibbs, and S.A. Siegelbaum. 1996. Subunit stoichiometry of cyclic nucleotide-gated channels and effects of subunit order on channel function. *Neuron.* 16:983–990.

Liu, D.T., G.R. Tibbs, P. Paoletti, and S.A. Siegelbaum. 1998. Constraining ligand-binding site stoichiometry suggests that a cyclic nucleotide-gated channel is composed of two functional dimers. *Neuron.* 21:235–248.

Maruyama, T., T. Kanaji, S. Nakade, T. Kanno, and K. Mikoshiba. 1997. 2APB, 2-aminoethoxydiphenyl borate, a membrane-penetrable modulator of Ins(1,4,5)P3-induced Ca^{2+} release. *J. Biochem. (Tokyo).* 122:498–505.

Matsushita, M., J.A. Kozak, Y. Shimizu, D.T. McLachlin, H. Yamaguchi, F.Y. Wei, K. Tomizawa, H. Matsui, B.T. Chait, M.D. Cahalan, and

A.C. Nairn. 2005. Channel function is dissociated from the intrinsic kinase activity and autophosphorylation of TRPM7/CHAK1. *J. Biol. Chem.* 80:20793–20803.

Monteilh-Zoller, M.K., M.C. Hermosura, M.J. Nadler, A.M. Scharenberg, R. Penner, and A. Fleig. 2003. TRPM7 provides an ion channel mechanism for cellular entry of trace metal ions. *J. Gen. Physiol.* 121:49–60.

Montell, C. 2005. The TRP superfamily of cation channels. *Sci. STKE.* 2005:re3.

Nadler, M.J., M.C. Hermosura, K. Inabe, A.L. Perraud, Q. Zhu, A.J. Stokes, T. Kurosaki, J.P. Kinet, R. Penner, A.M. Scharenberg, and A. Fleig. 2001. LTRPC7 is a Mg.ATP-regulated divalent cation channel required for cell viability. *Nature.* 411:590–595.

Nilius, B., T. Voets, and J. Peters. 2005. TRP channels in disease. *Sci. STKE.* 2005:re8.

Owsianik, G., K. Talavera, T. Voets, and B. Nilius. 2005. Permeation and selectivity of TRP channels. *Annu. Rev. Physiol.* [Epub ahead of print]

Prakriya, M., and R.S. Lewis. 2001. Potentiation and inhibition of Ca^{2+} release-activated Ca^{2+} channels by 2-aminoethyldiphenyl borate (2-APB) occurs independently of IP(3) receptors. *J. Physiol.* 536:3–19.

Reeh, P.W., and K.H. Steen. 1996. Tissue acidosis in nociception and pain. *Prog. Brain Res.* 113:143–151.

Runnels, L.W., L. Yue, and D.E. Clapham. 2001. TRP-PLIK, a bifunctional protein with kinase and ion channel activities. *Science.* 291:1043–1047.

Runnels, L.W., L. Yue, and D.E. Clapham. 2002. The TRPM7 channel is inactivated by PIP(2) hydrolysis. *Nat. Cell Biol.* 4:329–336.

Ryazanova, L.V., M.V. Dorovkov, A. Ansari, and A.G. Ryazanov. 2004. Characterization of the protein kinase activity of TRPM7/ChaK1, a protein kinase fused to TRP ion channel. *J. Biol. Chem.* 279:3708–3716.

Schlingmann, K.P., and T. Gudermann. 2005. A critical role of TRPM channel-kinase for human magnesium transport. *J. Physiol.* 566:301–308.

Schlingmann, K.P., S. Weber, M. Peters, L. Niemann Nejsum, H. Vitzthum, K. Klingel, M. Kratz, E. Haddad, E. Ristoff, D. Dinour, et al. 2002. Hypomagnesemia with secondary hypocalcemia is caused by mutations in TRPM6, a new member of the TRPM gene family. *Nat. Genet.* 31:166–170.

Schlingmann, K.P., M.C. Sassen, S. Weber, U. Pechmann, K. Kusch, L. Pelken, D. Lotan, M. Syrrou, J.J. Prebble, D.E.C. Cole, et al. 2005. Novel TRPM6 mutations in 21 families with primary hypomagnesemia and secondary hypocalcemia. *J. Am. Soc. Nephrol.* 16:3061–3069.

Schmitz, C., A.L. Perraud, C.O. Johnson, K. Inabe, M.K. Smith, R. Penner, T. Kurosaki, A. Fleig, and A.M. Scharenberg. 2003. Regulation of vertebrate cellular Mg2+ homeostasis by TRPM7. *Cell.* 114:191–200.

Schmitz, C., A.L. Perraud, A. Fleig, and A.M. Scharenberg. 2004. Dual-function ion channel/protein kinases: novel components of vertebrate magnesium regulatory mechanisms. *Pediatr. Res.* 55:734–737.

Schmitz, C., M.V. Dorovkov, X. Zhao, B.J. Davenport, A.G. Ryazanov, and A.L. Perraud. 2005. The channel kinases TRPM6 and TRPM7 are functionally non-redundant. *J. Biol. Chem.* 280:37763–37771.

Strubing, C., G. Krapivinsky, L. Krapivinsky, and D.E. Clapham. 2001. TRPC1 and TRPC5 form a novel cation channel in mammalian brain. *Neuron.* 29:645–655.

Strubing, C., G. Krapivinsky, L. Krapivinsky, and D.E. Clapham. 2003. Formation of novel TRPC channels by complex subunit interactions in embryonic brain. *J. Biol. Chem.* 278:39014–39019.

Takezawa, R., C. Schmitz, P. Demeuse, A.M. Scharenberg, R. Penner, and A. Fleig. 2004. Receptor-mediated regulation of the TRPM7 channel through its endogenous protein kinase domain. *Proc. Natl. Acad. Sci. USA.* 101:6009–6014.

Voets, T., J. Prenen, A. Fleig, R. Vennekens, H. Watanabe, J.G. Hoenderop, R.J. Bindels, G. Droogmans, R. Penner, and B. Nilius. 2001. CaT1 and the calcium release-activated calcium channel manifest distinct pore properties. *J. Biol. Chem.* 276:47767–47770.

Voets, T., B. Nilius, S. Hoefs, A.W.C.M. van der Kemp, G. Droogmans, R.J.M. Bindels, and J.G.J. Hoenderop. 2004. TRPM6 forms the Mg^{2+} influx channel involved in intestinal and renal Mg^{2+} absorption. *J. Biol. Chem.* 279:19–25.

Walder, R.Y., D. Landau, P. Meyer, H. Shalev, M. Tsolia, Z. Borochowitz, M.B. Boettger, G.E. Beck, R.K. Englehardt, R. Carmi, and V.C. Sheffield. 2002. Mutation of TRPM6 causes familial hypomagnesemia with secondary hypocalcemia. *Nat. Genet.* 31:171–174.

Wang, R., J. Su, X. Wang, H. Piao, X. Zhang, C.Y. Adams, N. Cui, and C. Jiang. 2005. Subunit stoichiometry of the Kir1.1 channel in proton-dependent gating. *J. Biol. Chem.* 280:13433–13441.

Wicher, D., H.-J. Agricola, R. Schonherr, S.H. Heinemann, and C. Derst. 2005. TRPγ channels are inhibited by cAMP and contribute to pacemaking in neurosecretory insect neurons. *J. Biol. Chem.* 281:3227–3236.

Wu, J., N. Kamimura, T. Takeo, S. Suga, M. Wakui, T. Maruyama, and K. Mikoshiba. 2000. 2-Aminoethoxydiphenyl borate modulates kinetics of intracellular Ca^{2+} signals mediated by inositol 1,4,5-trisphosphate-sensitive Ca^{2+} stores in single pancreatic acinar cells of mouse. *Mol. Pharmacol.* 58:1368–1374.

Xu, S.Z., F. Zeng, G. Boulay, C. Grimm, C. Harteneck, and D.J. Beech. 2005. Block of TRPC5 channels by 2-aminoethoxydiphenyl borate: a differential, extracellular and voltage-dependent effect. *Br. J. Pharmacol.* 145:405–414.

Yermolaieva, O., A.S. Leonard, M.K. Schnizler, F.M. Abboud, and M.J. Welsh. 2004. Extracellular acidosis increases neuronal cell calcium by activating acid-sensing ion channel 1a. *Proc. Natl. Acad. Sci. USA.* 101:6752–6757.

Yue, L., J.L. Feng, Z. Wang, and S. Nattel. 2000. Effects of ambasilide, quinidine, flecainide and verapamil on ultra-rapid delayed rectifier potassium currents in canine atrial myocytes. *Cardiovasc. Res.* 46:151–161.

Yue, L., P. Melnyk, R. Gaspo, Z. Wang, and S. Nattel. 1999. Molecular mechanisms underlying ionic remodeling in a dog model of atrial fibrillation. *Circ. Res.* 84:776–784.

Yue, L., J.B. Peng, M.A. Hediger, and D.E. Clapham. 2001. CaT1 manifests the pore properties of the calcium-release-activated calcium channel. *Nature.* 410:705–709.

Yue, L., B. Navarro, D. Ren, A. Ramos, and D. Clapham. 2002. The cation selectivity filter of the bacterial sodium channel, NaChBac. *J. Gen. Physiol.* 120:845–853.

Zheng, J., and F.J. Sigworth. 1998. Intermediate conductances during deactivation of heteromultimeric Shaker potassium channels. *J. Gen. Physiol.* 112:457–474.